# Quasionedimensional quantum wells

Rolando Pérez-Álvarez. Departamento de Física Teórica, Universidad de La Habana, Cuba

**RESUMEN**

Se estudian los estados electrónicos y propiedades ópticas de pozos cuánticos cuasiunidimensionales usando la Aproximación de la Función Envolvente en un modelo a una banda. Se deducen las condiciones de contorno que deben satisfacer la función envolvente radial. Se obtiene la ecuación trascendente para los niveles de energía así como la función de onda normalizada y el confinamiento en la aproximación de banda plana considerando un perfil de masa seccionalmente constante. Obtenemos también una expresión general para el coeficiente de absorción de un cable cuántico. Se reportan las reglas de selección correspondientes. La fórmula así obtenida es aplicada a los casos de sección transversal rectangular y circular, y barrera de potencial infinita. Damos resultados numéricos para el pozo cuántico de GaAs-$Al_xGa_{1-x}As$ (x=0,32).

**ABSTRACT**

Using the Envelope Function Approximation and a one band model the electronic states and optical properties of quasionedimensional quantum wells are studied. The boundary conditions to be fulfilled by the radial envelope

functions are deduced. The transcendental equation for the energy levels, the normalised wave functions and the confinement are obtained in the flat band approximation considering a sectionally constant mass profile. We obtain also a general expression for the absorption coefficient of a quantum wire. The corresponding selection rules are reported. The formula just obtained is applied to the cases of rectangular and circular cross section and infinite potential barrier. Numerical results for the GaAs-$Al_xGa_{1-x}As$(x=0,32) quantum well are given.

## 1. INTRODUCTION

In the last 15 years the apparition of new experimental techniques has made possible the construction of ultrathin multilayer systems made up by semiconductors /1/. These systems are characterized by the confinement of the carrier motion to a very thin region in one direction, the other two directions remaining free. In this way we obtain a quasitwodimensional (quasi-2D) electronic system.

More recently lower dimensional quantum wells (QW) and superlattices (SL) have been studied. In /2-6/ quasionedimensional (quasi-1D) systems are proposed. In /7-11/ they are constructed and experimentally analized.

These new systems exhibit certain features which make them useful as semiconductor devices. Among them we have that the energy levels, gaps, effective masses and other parameters can be taylored practically. They show negative resistivities, large mobilities, etc. Other interesting physical properties could be expected such as charge instability and Kohn's anomaly.

These successes have stimulated the theoretical study of the electronic states /12-15/, excitonic states /16/, impurity states /17-19/, as well as the electric /20-28/ and optical /29,30/ properties.

In most part of the papers listed here the QW of GaAs-$Al_xGa_{1-x}As$ are studied, Nevertheless in other papers quasi-1D QW based on ultrathin inversion channels of Si-$SiO_2$ are studied.

Some groups have begun to construct low dimensional systems in the form of ribbons /31/, disks /7,31/ and boxes or drops /9-11/.

In the present paper we pay attention to the electronic states and optical interband properties of quasi-1D QW.

In the second and third sections we analize the electronic states of a cylindrical QW (Fig. 1) in the flat band approximation considering finite potential barriers and sectionally constant effective mass. If the depth of the well is taken infinite the problem is easier and is already solved

/32/. In /6,32/ the problem for the well of finite depth and constant mass is solved. Our results reproduce these particular cases.

In the section 4 the energy levels and the confinement of a GaAs-$Al_{0,32}Ga_{0,68}As$ QW are given as a function of the QW radius.

In section 5 we deduce a general expression for the allowed interband and intraband absorption coefficient of a quantum wire with arbitrary cross section and the selection rules for these transitions are given. This expression is applied in section 6 to the particular cases of rectangular and circular cross sections. The section 7 is devoted to present the numerical results for the absorption coefficient.

Finally, in section 8 we summarize our results and establish some conclusions.

All the calculations are made in the framework of one band Envelope Function Approximation (EFA).

## 2. SCHRODINGER EQUATION WITH VARIABLE MASS IN CYLINDRICAL SYMMETRIC SYSTEM

The quantum mechanical model we use is a system in which the effective mass is $m(\rho)$ and the potential is $V(\rho)$. Both functions only depend on the cylindrical variable $\rho$. The equation for the envelope function is then /33/:

$$\{1/2\ \hat{\vec{p}}.(1/m(\rho)\hat{\vec{p}}) + V(\rho)\}\psi(\vec{r}) = E\ \psi(\vec{r}) \qquad (1)$$

This problem can be solved by separating variables; so:

$$\psi(\rho,\theta,z) = R(\rho)\ \Theta_n(\theta) Z_{k_z}(z) \qquad (2)$$

$$\Theta_n(\theta) = \frac{1}{(2\pi)^{1/2}}\ e^{in\theta} \qquad n = 0,1,2... \qquad (3)$$

$$Z_{k_z}(z) \frac{1}{(2\pi)^{1/2}}\ e^{ik_z z} \qquad (4)$$

obtaining for the radial part the equation

$$R''(\rho) + \frac{m(\rho)}{\rho}\ \frac{d}{d\rho}\left[\frac{\rho}{m(\rho)}\right] R'(\rho) + \left[k^2 - \frac{n^2}{\rho^2}\right] R(\rho) = 0 \qquad (5)$$

$$k^2 = \frac{2m(\rho)}{\hbar^2}\ (E-V(\rho)) - k_z^2 \qquad (6)$$

As usually we take $R(\rho)$ continuous. From (5) it is easy to deduce that its derivative satisfies a condition rather more complex, i.e.:

$$\frac{R'(\rho+)}{m(\rho+)} = \frac{R'(\rho-)}{m(\rho-)} \qquad (7)$$

that is: where $m(\rho)$ is continuous $R'(\rho)$ is continuous too; but a jump in $m(\rho)$ will produce a jump in $R'(\rho)$. A similar property is found in layered QW and SL /34,35/ and the deduction is very similar (we integrate equation (5) from $\rho-\varepsilon$ to $\rho+\varepsilon$ and then take the limit when $\varepsilon \to 0$).

Adequate boundary conditions have to be added to this equation to determine the solutions of physical interest. Particularly if we search for stationary states of the discrete spectrum, it is necessary to impose $R(\rho)$ to be finite for all $\rho$ and $\rho^{\frac{1}{2}}R(\rho)$ to be square integrable in $(0,\infty)$.

Notice that if $m(\rho)=M=$const., the longitudinal and radial motions are decoupled and the energy depends on $k_z$ in a simple form:

$$E_{\nu n}(k_z) = \epsilon_{\nu n} + \frac{\hbar^2 k_z^2}{2M} \tag{8}$$

where $\nu$ is the index that labels the levels for a given $\mu$. If $m(\rho)$ is not constant, this decoupling is not possible.

## 3. SECTIONALLY CONSTANT MASS AND POTENTIAL

Let us suppose that

$$V(\rho) = \begin{cases} V_1 & \rho < a \\ V_2 & \rho > a \end{cases} \tag{9}$$

$$m(\rho) = \begin{cases} m_1 & \rho < a \\ m_2 & \rho > a \end{cases} \tag{10}$$

and denote

$$k_3^2 = -k_3^2 = \frac{2m_j}{\hbar^2}(E-V_j) - k_z^2 \qquad j=1,2 \tag{11}$$

Then we have that

$$R''(\rho) + \frac{1}{\rho} R'(\rho) + \left[k_3^2 - \frac{n^2}{\rho^2}\right] R(\rho) = 0 \tag{12}$$

with $j=1$ if $\rho < a$ and $j=2$ if $\rho > a$.

This inequalities are obtained in particular if $k_z=0$ and $V_1 < E < V_2$.

Thus we shall obtain a Bessel equation for $\rho<a$ and a Bessel equation of imaginary argument for $\rho > a$ /36/, therefore:

$$R(\rho) = \begin{cases} AJ_n(k_1\rho) + BN_n(k_1\rho) \\ CI_n(k_2\rho) + DK_n(K_2\rho) \end{cases} \tag{13}$$

with the conditions

$$|R(0)| < \infty \tag{14}$$

$$|R(\infty)| < \infty \tag{15}$$

that implies B=C=0.

Applying the matching conditions

$$R(a+) = R(a-) \tag{16}$$

$$\frac{R'(a+)}{m(a+)} = \frac{R'(a-)}{m(a-)} \tag{17}$$

and the normalization of the wave function

$$\int_0^\infty d\rho\ \rho\ R^2(\rho) = 1 \tag{18}$$

it is not difficult to conclude that the allowed energy values are obtained from the transcendental equation:

$$J_n(k_1 a) K_n'(k_2 a) - \frac{k_1}{k_2}\frac{m_2}{m_1} J_n'(k_1 a) K_n(k_2 a') = 0 \tag{19}$$

while

$$A = \frac{2^{\frac{1}{2}}}{a|J_n(k_1 a)|} \sqrt{\frac{1}{\frac{K_{n-1}(k_2 a)K_{n+1}(k_2 a)}{K_n^2(k_2 a)} - \frac{J_{n-1}(k_1 a)J_{n+1}(k_1 a)}{J_n^2(k_1 a)}}} \tag{20}$$

$$D = A\,\frac{J_n(k_1 a)}{K_n(k_2 a)} \tag{21}$$

If the energy level is very close to the top of the well, the argument of $K_n$ and $K_n'$ becomes very small, while the one of $J_n$ and $J_n'$ approaches to

$$x_B = \sqrt{\frac{2m_1}{\hbar^2}(V_2 - V_1)a^2} \tag{22}$$

This consideration allows us to find a transcendental equation whose solution gives the values of a for which a new level with a given n (n > 1) appears:

$$J_n(x_B) - \lambda\, x_B\, J_{n-1}(x_B) = 0 \tag{23}$$

$$1/\lambda = n\left[1 - \frac{m_1}{m_2}\right] \tag{24}$$

The first roots of this equation can be seen in /36/.

For large a, the use of the asymptotic form of $J_n(x_B)$ allows us to give an explicit expression for the radius:

$$x_{B\nu n} = \pi/4\ (1 + 2n + 4\nu) + d_n \qquad (25)$$

$$d_n = \operatorname{arctg}\left\{n\left[\frac{m_1}{m_2} - 1\right]\right\} \qquad -\pi/2 < d_n < \pi/2 \qquad (26)$$

($\nu$ labels the different solutions of (23)-(24)).

We calculate also, as an interesting quantity, the probability for the particle to be inside the cylinder in a stationary state. We call this parameter *confinement*, and as a result of the calculation performed we obtained that:

$$C_{\nu n}(k_z) = \left[1 - \frac{1 - \dfrac{K_{n-1}(k_2 a) K_{n+1}(k_2 a)}{K_n^2(k_2 a)}}{1 - \dfrac{J_{n-1}(k_1 a) J_{n+1}(k_1 a)}{J_n^2(k_1 a)}}\right]^{-1} \qquad (27)$$

## 4. NUMERICAL RESULTS

We use the following parameters for the GaAs-$Al_xGa_{1-x}As$ cylindrical QW /37/:

| | |
|---|---|
| Conduction band (CB) | $m_1 = 0{,}0665\text{-}m_0$ |
| | $m_2 = m_1 + 0{,}0835 \times m_0$ |
| | $V_2 - V_1 = r\Delta E_g$ |
| Valence band. Heavy holes (HH) | $m_1 = 0{,}45\ m_0$ |
| | $m_2 = m_1 + 0{,}302 \times m_0$ |
| | $V_2 - V_1 = (1-r)\ \Delta E_g$ |
| Valence band. Light holes (LH) | $m_1 = 0{,}08\ m_0$ |
| | $m_2 = m_1 + 0{,}057 \times m_0$ |
| | $V_2 - V_1 = (1-r)\ \Delta E_g$ |

Here $m_0$ is the free electron mass, $\Delta E_g$ is the difference between the gaps of $Al_xGA_{1-x}As$ and GaAs (0,4 eV for x=0,32), r is the rule for CB offset in between the materials (r=0,6 /38/).

In Fig. 2 the results for the energy levels of the bands as a function of the radius of the well are shown. In Fig. 3 the results for the confinement are depicted. In both cases x=0,32 and a varies from 0 to $1000a_0$. Obviously, when a is close to zero the EFA does not work any more; we calculate this region in order to control our results.

It is interesting to note that (25)-(26) give the value of a with a maximum error of 10 % with respect to the exact one obtained from (19). The calculation of Bessel functions was made with the polynomial and assymptotic expressions /36/ which guarantee an error less than $10^{-6}$.

## 5. $\alpha(\omega)$ FOR A QUANTUM WIRE WITH ARBITRARY CROSS SECTION

In the frame of envelope function approximation, for a 1D QW the wave function has the form:

$$\psi(\vec{r}) = \frac{e^{ik_z z}}{(2\pi)^{\frac{1}{2}}} F(\vec{\rho})\ u(\vec{r}) \tag{28}$$

where we have written $\vec{r} = (\vec{\rho}, z)$, $L_z$ is the lenght of the wire, $k_z$ the wave vector along the z axis, F the plane part of the envelope function and u is the periodic part of the Bloch function.

On the other hand, the optical absorption coefficient is equal to:

$$\alpha(\omega) = \alpha_0 \sum_{i,f} \frac{1}{m_0} |\langle f|\vec{e}.\vec{p}|i\rangle|^2 \delta(E_f - E_i - \hbar\omega)\ [f(E_i) - f(E_f)] \tag{29}$$

f(E) is the Fermi-Dirac distribution function and the index i (f) denotes the initial (final) state. $\vec{p} = -i\hbar\nabla$ is the momentum operator and $\vec{e}$ is the polarization vector of the light.

In order to calculate the matrix element of the momentum operator we adopt the form (28) for $\langle\vec{r}|f\rangle$ and $\langle\vec{r}|i\rangle$. Taking into account the rapid variation of u inside the unit cell, whereas F varies slowly, we can make the following approximation:

$$\langle f|\vec{e}.\vec{p}|i\rangle = \delta_{k_{zf},k_{zi}} \{\vec{e}.\vec{K}_{if} S_{if} + \delta_{\nu_i,\nu_f} \vec{e}_\perp . \vec{\Pi}_{if}\} \tag{30}$$

where

$$\vec{K}_{if} = \frac{1}{V_0} \int_{V_0} d\vec{r}\ u_f^*(\vec{r})\ \vec{p}\ u_i(\vec{r}) \tag{31}$$

$V_0$ is the unit cell,

$$S_{if} = \int_S d\vec{\rho}\ F_f^*(\vec{\rho})\ F_i(\vec{\rho}) \tag{32}$$

S is the plane perpendicular to the z axis,

$$\vec{\Pi}_{if} = \int_S d\vec{\rho}\, F_f^*(\vec{\rho})\, \hat{\vec{p}}_i F_i(\vec{\rho}) \tag{33}$$

$$\vec{p} = (\vec{p}_\perp, p_z) = (\vec{p}_\perp, -i\hbar \frac{\partial}{\partial z})$$

$$\vec{e} = (\vec{e}_\perp, e_z)$$

and $\nu$ is the band index.

The first term on the r.h.s. of (30) is associated with interband transition because the second vanishes for $\nu_i \neq \nu_f$. Note that in this case the overlap integral $S_{if}$ is the relevant magnitude. The corresponding selection rules are:

i) $E_f = E_i + \hbar\omega$

ii) $k_{zf} = k_{zi}$

iii) $\vec{e}.\vec{K}_{if} \neq 0$.

iv) $S_{if} \neq 0$

The second term on the r.h.s. of (30) is associated with intraband (intersubband) transitions. Now the relevant quantity is the matrix element between envelope functions, $\vec{e}.\vec{\Pi}_{if}$. The selection rules are formulated as follows:

1) $E_f = E_i + \hbar\omega$

2) $k_{zf} = k_{zi}$

3) $\vec{e}.\vec{\Pi}_{if} \neq 0$

In order to obtain $\alpha(\omega)$ we substitute (30)-(33) in (29) and sum over $i=(\nu_i, k_{zi}, n_i)$ and $f=(\nu_f, k_{zf}, n_f)$, where $n_i$ ($n_f$) is the index identifying the plane part of the envelope function for the initial (final) state.

Finally we obtain for the transitions between two bands:

$$\alpha(\omega) = \alpha_0 \frac{|\vec{e}.\vec{K}|^2}{m_0} \frac{L_z}{2\pi} \sum_{n_i, n_f} \left| \frac{2|S_{if}|^2}{\frac{d(E_f - E_i)}{dk_z}} \right|_{k_{z\omega}} [f(E_i) - f(E_f)] \tag{34}$$

while for the intersubband transitions we have:

$$\alpha(\omega) = \alpha_0 \frac{L_z}{2\pi} \sum_{n_i,n_f} \frac{|\vec{e}_\perp \cdot \vec{\Pi}_{if}|^2/m_0}{\left|\frac{d(E_f-E_i)}{dk_z}\right|_{k_{z\omega}}} [f(E_i)-f(E_f)] \tag{35}$$

In both cases $k_{z\omega}$ is such that

$$(E_f - E_i)_{k_{z\omega}} = \hbar\omega \tag{36}$$

## 6. RECTANGULAR AND CIRCULAR CROSS SECTION

For the 1D QW with rectangular cross section and infinite potential barriers we have:

$$F(\vec{\rho}) = \frac{2}{\sqrt{L_x L_y}} \sin \frac{n_x \pi x}{L_x} \sin \frac{n_y \pi y}{L_y} \tag{37}$$

$$E_{n_x,n_y} = \frac{\hbar^2 k_z^2}{2m^*} + \frac{\hbar^2\pi^2}{2m^*} [(n_x/L_x)^2 + (n_y/L_y)^2] + V_i \tag{38}$$

$$n_x, n_y = 1,2,3,\ldots$$

$m^*$ is the effective mass of the band under consideration.

A simple calculation yields:

$$S_{if} = \delta_{n_{xi},n_{xf}} \delta_{n_{yi},n_{yf}} \tag{39}$$

$$\vec{e}_\perp \cdot \vec{\Pi}_{if} = -2i\hbar \left[ \frac{n_{xf}}{L_x} \delta_{n_{yf},n_{yi}} e_x A_{n_{xi},n_{xf}} + \frac{n_{yf}}{L_y} \delta_{n_{xi},n_{xf}} e_y A_{n_{yi},n_{yf}} \right] \tag{40}$$

$A_{pq} = 0$ for $p = q$, while for $p \neq q$ we have:

$$A_{pq} = \frac{p}{p^2-q^2} [1-(-1)^{p+q}] \tag{41}$$

Hassan and Spector's results /29/ for the interband absorption coefficient can be obtained directly from (34) and (39):

$$\alpha(\omega) = \alpha_0 \frac{|\vec{e}\cdot\vec{K}|^2}{m_0} \frac{L_z}{2\pi} \sqrt{\frac{\mu}{2\hbar^2}} \sum_{1,m} \frac{[f(E_i)-f(E_f)]}{\sqrt{\hbar\omega - E_g - \frac{\hbar^2\pi^2}{2\mu}\left[\left(\frac{n_x}{L_x}\right)^2 + \left(\frac{n_y}{L_y}\right)^2\right]}} \tag{42}$$

where $\mu$ is the reduced mass and $E_g$ the energy gap between the two bands under consideration.

Now we have the additional selection rules:

iv.a) $\Delta n_x = 0$

iv.b) $\Delta n_y = 0$

3.a) if $e_x \neq 0$, then $\Delta n_x \neq 0$ and $n_y$ must change its parity.

3.b) if $e_y \neq 0$, then $\Delta n_y \neq 0$ and $n_x$ must change its parity.

For the 1D QW with circular cross section, infinite barrier and radius a, the envelope functions are zero for $\rho > a$, while for $\rho < a$, they have the form:

$$F_{lm}(\rho) = A \frac{e^{im\varphi}}{\sqrt{2\pi}} J_m(k\rho) \tag{43}$$

The energy levels are:

$$E_{lm}(k_z) = \frac{\hbar^2 k_z^2}{2m^*} + \frac{\hbar^2 x_{lm}^2}{2m^* a^2} + V_1 \tag{44}$$

$$m = 0,1,2,\ldots \; ; \quad l = 1,2,3,\ldots$$

$$A = \frac{\sqrt{2}}{a} \frac{1}{[J'_m(ka)]} \tag{45}$$

$$k = \sqrt{\frac{2m^*}{\hbar^2} E_{lm} - k_z^2} \tag{46}$$

where the energies are measured from the bottom of the well and $x_{lm}$ is the l-th root of the Bessel function $J_m(x)$.

It is not difficult in this case to obtain the following results:

$$S_{if} = \delta_{m_i,m_f} \, \delta_{l_i,l_f} \tag{47}$$

$$\frac{|\vec{e}_1 \cdot \vec{\pi}_{if}|^2}{m_0} = \frac{\hbar^2 e}{4 m_0 a^2} M_{m_i,m_f} \tag{48}$$

$$B_{m_i,m_i+1} = ((m_i+1)I_1 + I_2)^2$$

$$B_{m_i,m_i-1} = ((m_i-1)I_1 - I_2)^2$$

and $B_{m_i,m_f} = 0$ otherwise. We have used the notations:

$$I_1 = \int_0^1 dx\, J_{m_i}(\alpha x)\, J_{m_f}(\beta x) \tag{49}$$

$$I_2 = \int_0^1 dx\, x\, J_{m_i}(\alpha x)\, \frac{dJ_{m_f}(\beta x)}{dx} \tag{50}$$

$$\alpha = k_i a \tag{51}$$

$$\beta = k_f a \tag{52}$$

From the last expressions we may directly derive the following selection rules:

iv.a) $\Delta m = 0$

iv.b) $\Delta l = 0$

3) $m_f = m_i + 1$ or $m_f = m_i - 1$

Finally, for the absorption coefficient for interband transitions we obtain:

$$\alpha(\omega) = \alpha_0 \frac{|\vec{e}.\vec{K}|^2}{m_0} \frac{L_z}{2\pi} \sqrt{\frac{\mu}{2\hbar^2}} \sum_{l,m} \frac{[f(E_i)-f(E_f)]}{\sqrt{\hbar\omega - E_g - \frac{\hbar^2 x_{lm}^2}{2\mu a^2}}} \tag{53}$$

As in the rectangular case, in order to consider the intraband transitions we should introduce phenomenologically a relaxation parameter /30/. We do not consider this effect.

## 7. NUMERICAL RESULTS

In Fig. 4 we present the curve $\alpha(\omega)$ associated with the transitions between the conduction band and the heavy hole band for a GaAs cylindrical wire. The conduction band is assumed to be completely empty whereas the valence band is assumed to be full. The corresponding effective masses are $m_c^* = 0{,}0665 m_0$ and $m_v^* = 0{,}45 m_0$, $m_0$ being the free electron mass. As can be seen from the figure, the curve for the circular cross section is very similar to that for the rectangular cross section /30/. The calculations were carried out for $a/a_0 = 200$, $a_0$ being the Bohr's radius.

## 8. CONCLUSIONS

The matching conditions for the cylindrical symmetry are reported for the first time taken into account a position dependent mass.

The transcendental equation for the energy levels of the cylindrical well with finite depth and variable mass is obtained when both functions -potential and mass- are sectionally constant.

The confinement of the charge carriers is also calculated for this case. This magnitude gives a criterion of the validity of the infinite well approach (completely confined states) to calculate the energy levels in the QW.

We report numerical results for a typical and interesting case: a cylinder of GaAs in a $Al_{0,32}Ga_{0,68}As$ matrix.

As in layered structures, we find significatives differences in all the magnitudes calculated when the mass mistmach and/or the finite depth is taken into account for the levels not too close to the bottom of the well.

From Fig. 3 it can be seen that the states are rapidly confined whitin the well when the radius increases.

These numerical results for typical values of the parameters allows to conclude that the approximation of the infinito well is a good one to study the lowest levels when they are close to the bottom.

The main results of this work concerning the optical properties of quasi 1D systems are the formulae (34)-(35) for the absorption coefficient $\alpha(\omega)$ and the corresponding selection rules i)-iv) and 1)-3) for the interband and intraband transitions respectively. These formulae may be used to calculate the absorption coefficient of superlattices /12/ and QW wires.

Also as a main result, we have given the dependence of $\alpha(\omega)$ for the quantum wire with circular cross section and infinite potential barrier, and the corresponding selection rules. The absorption coefficient for this system has singularities at the photon energies

$$\hbar\omega_{1m} = E_g + \frac{\hbar^2 x_{1m}^2}{2\mu a^2} \qquad (54)$$

The optical edge is shifted to higher energies by the amount $\hbar^2 x_{10}^2/2\mu a^2$. If we take a square well, the corresponding shift is $\hbar^2\pi^2/2\mu L^2$. This implies that if we made these two wires with the same quantity of material ($\pi a^2 = 1^2$) and measured its absorption spectrum, we would find that the edge of the circular wire is shifted $x_{10}^2/\pi = 1,8$ times with respect to the square one.

In principle the assumption that the carriers are completely confined is not so strong. In sections 2-4 it was shown that the carriers are rapidly confined when we increases the radius of the cylinder. This analysis

may justify the application of our results to practical cases when we study the first absorption singularities.

Different parts of this work have been published /39-41/. A more detailed analysis of the absorption coefficient of a GaAs-$Al_xGa_{1-x}As$ quantum wire will be submitted to publication in the near future.

ACKNOWLEDGEMENTS

The author would like to thank the IAEA and UNESCO for hospitality at the ICTP, Trieste, where part of this work was done. He is grateful to V. R. Velasco and F. García-Moliner from the CSIC, Spain, and to C. Trallero-Giner, H. Rodríguez-Coppola and J. López-Gondar from the University of Havana, Cuba, for helpful comments on the manuscript.

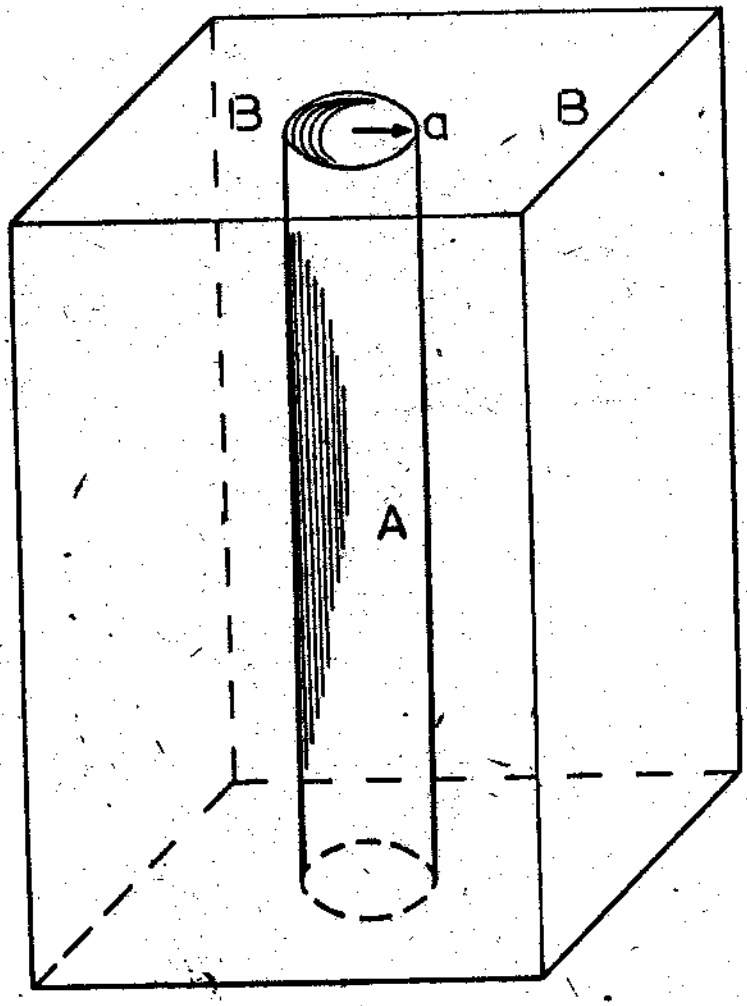


Figure 1. Cylindrical quantum well

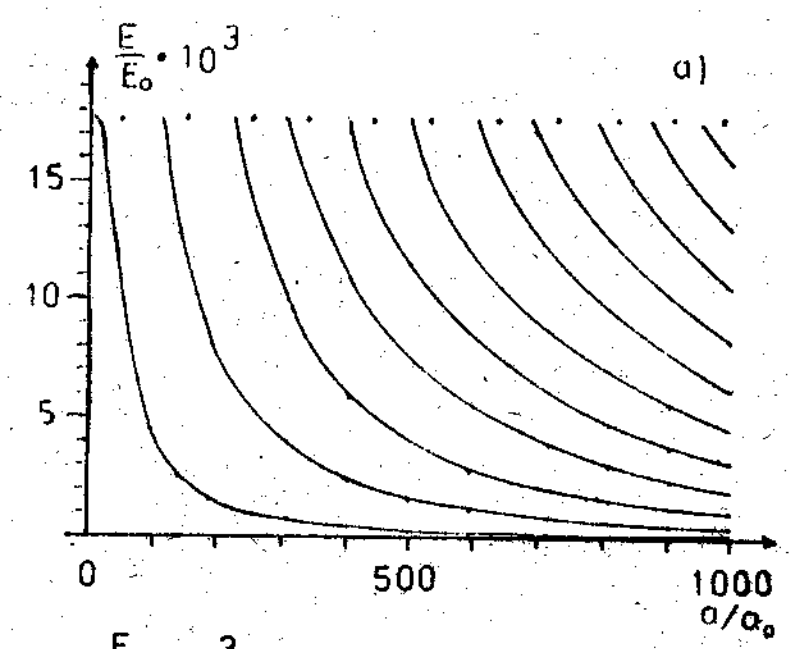


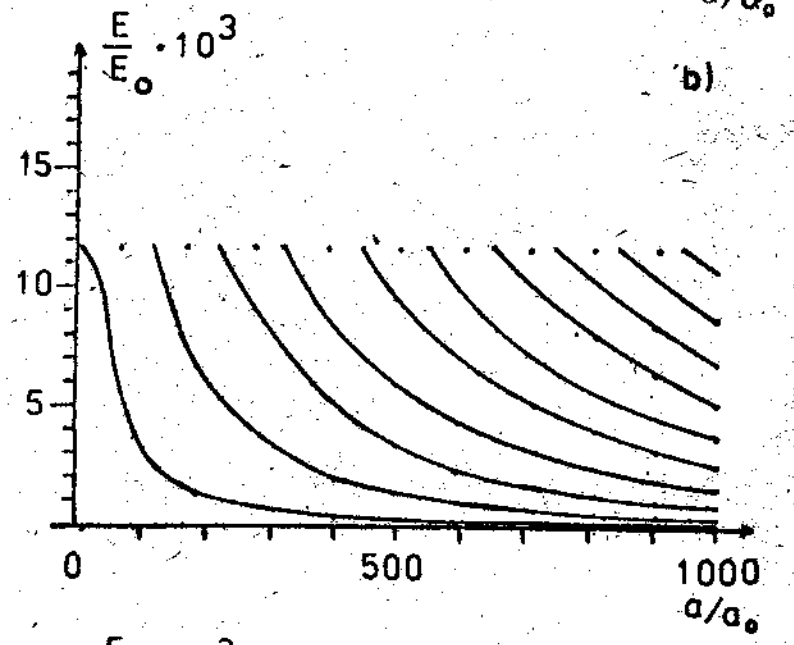


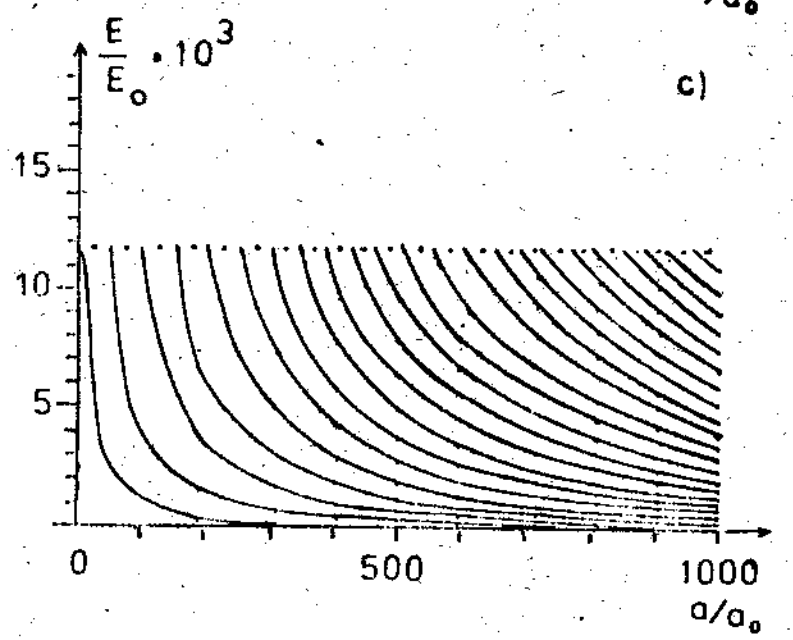


**Figure 2.** First energy levels (n=0) vs radius. We also show with small points the radius of appearence of the n=1 levels. $E_0$=13,60 eV=1 Ry, $a_0$=0,0529 nm is the Bohr's radius. a) CB; b) VB light holes; c) VB heavy holes.

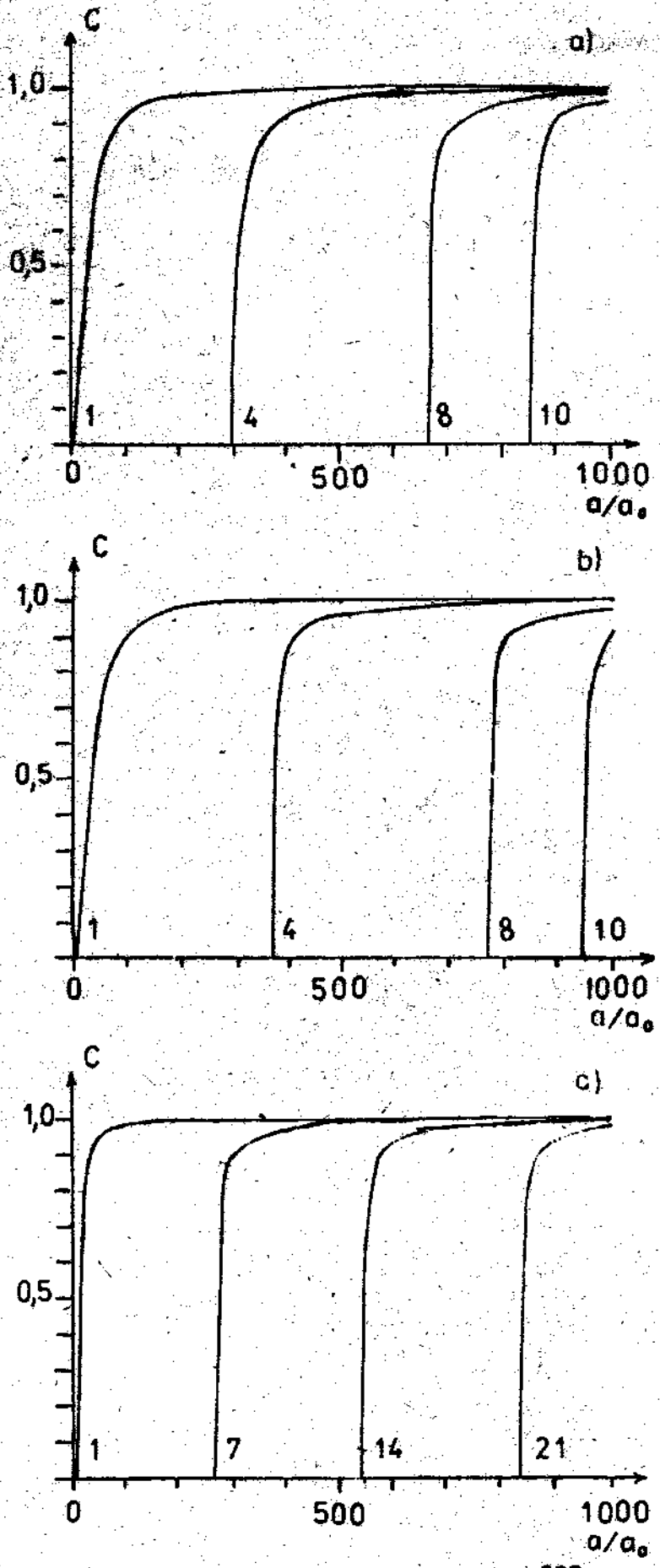


Figure 3. Confinement of some states for the three bands considered. a) CB; b) VB light holes; c) VB heavy holes. The quantum number $\nu$ is indicated. $n=0$ and $k_z=0$ in all cases.

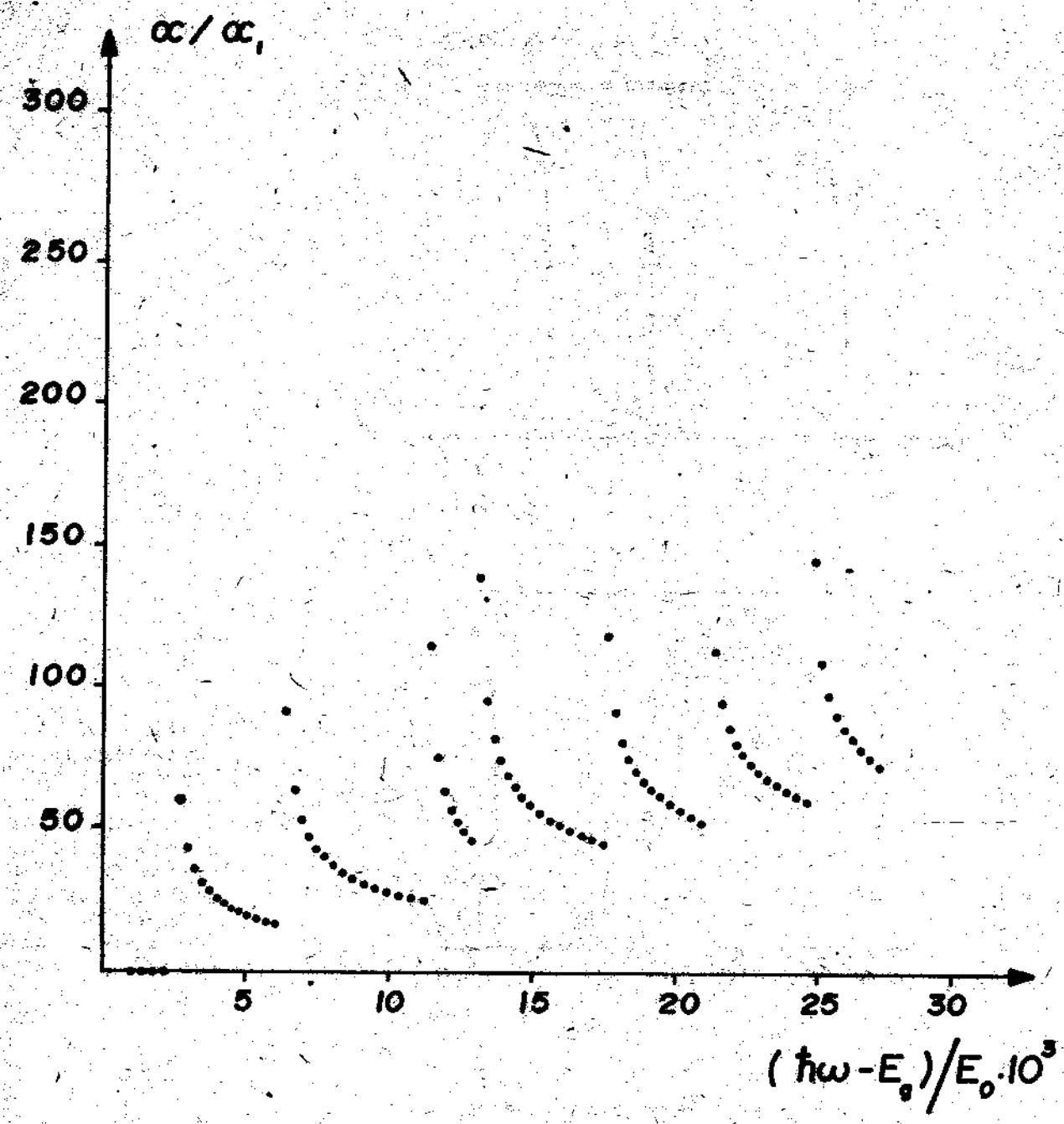


Figure 4. Absorption coefficient associated with the transitions between the conduction and heavy holes band for a QW wire of GaAs with circular cross section and infinite potential barrier, $\alpha_1$ is the prefactor in the r.h.s. of equation (53) when atomic units are taken.

1. Esaki, L.
J. de Physique Colloques C5, supplement au numero 2, Tome 45, C5-3 (1984).

2. Kazarinov, R. F. and R. A. Suris
Soviet Phys. Semic., v. 7, p. 347 (1973).

3. Sakaki, H.
Japn. J. Appl. Phys., v. 19, p. L735 (1980).

4. Bates, R. T.
Bull. Am. Phys. Soc., v. 22, p. 407 (1977).

5. Ferry, D. K.
Physica Status Solidi (b), v. 106, p. 63 (1981).

6. Iafrate, G. J., D. K. Ferry and R. K. Reich
Surf. Sci., v. 113, p. 485 (1982).

7. Holonyak, N. Jr., W. D. Laidig, M. D. Camras, J.J. Coleman and P.D.Dapkus
Appl. Phys. Lett., v. 39, p. 102 (1981).

8. Pettroff, P. M., A. C. Gossard, R. A. Logan and W. Wiegmann
Appl. Phys. Lett., v. 41, p. 635 (1982).

9. Cibert, J., P. M. Pettroff, G. J. Dolan, S. J. Pearton, A. C. Gossard and J. H. English
Appl. Phys. Lett., v. 49, p. 1275 (1986).

10. Reed, M. A., R. T. Bate, K. Bradshaw, W. M. Duncan, W. R. Frensley, J. W. Lee and H. D. Shih
J. Vac. Sci. Technol., v. B4, p. 358 (1986).

11. Miyamoto, Y., M. Cao, Y. Shingai, K. Furuya, Y. Suematsu, K. G. Ravikumar and S. Arai
Japn. J. Appl. Phys., v. 26, p. L225 (1987).

12. Wong, K. B., M. Jaros and J. P. Hagon
Phys. Rev. B, v. 35, p. 2463 (1987).

13. Brum, J. A., G. Bastard, L. L. Chang and L. Esaki
Submitted to publication.

14. Brum, J. A., G. Bastard, L. L. Chang and L. Esaki
Submitted to publication.

15. Lai, W. Y. and S. Das Sarma
Phys. Rev. B, v. 33, p. 8874 (1986).

16. Brown, J.W. and H.N. Spector.
Phys. Rev. B, v. 35, p. 3009 (1987).

17. Lee, J. and H. N. Spector
J. Vac. Sci. Technol., v. B2, p. 16 (1984).

18. Brum, J. A.
Submitted to Solid State Communications.

19. Osorio, F. A. P., M. H. Degani, and O. Hipolito
Submitted to publication.

20. Arora, V. K.
Physica Status Solidi (b), v. 105, p. 707 (1981).

21. Arora, V. K. and M. Prasad
Physica Status Solidi (b), v. 117, p. 127 (1983).

22. Comas, F., C. Trallero- Giner and J. Tutor
Physica Status Solidi (b), v. 139, p. 433 (1987).

23. Comas, F., C. Trallero-Giner, J. Tutor and H. Leon
To be published in Physica B & C.

24. Reich, R. K., R. O. Grondin and D. K. Ferry
Phys Rev. B, v. 27, p. 3483 (1983).

25. Lee, J. and H. N. Spector
J. Appl. Phys., v 54, p. 3921 (1983).

26. Lee, J. and M. O. Vassell
J. Phys. C, v. 17, p. 2525 (1984).

27. Fishman, G.
Phys. Rev. B, v. 34, p. 2394 (1986).

28. Sakaki, H.
J. Vac. Sci. Technol., v. 19, p. 148 (1981).

29. Hassan, H. H. and H. N. Spector
J. Vac. Sci. Technol., v. A3, p. 22 (1985).

30. Hassan, H. H. and H. N. Spector
Phys. Rev. B, v. 33, p. 5456 (1986).

31. Kash, K., A. Scherer, J. M. Worlock, H. G. Craighead and M. C. Tamargo
Appl. Phys. Lett., v. 49, p. 1043 (1986).

32. Galitskii, V. M., B. M. Karnakov and B. I. Kogan
*Problems in Quantum Mechanics*, Nauka, Moscow (1984), in russian.

33. Van Vliet, C. M. and A. H. Marshak
Phys. Rev. B, v. 29, p. 5960 (1984), and references therein.

34. Kroemer, H. and Zhu Qi-Gao
J. Vac. Sci. Technol., v. 21, p. 551 (1982).

35. Milanovic, M. and D. Tjapkin
Physica Status Solidi (b), v. 110, p. 687 (1982).

36. Abramowitz, M. and I. A. Stegun
*Handbook of Mathematical Functions*, Dover Publications Inc., N. Y. (1972).

37. Xu., Z. Y., V. K. Kreismanis and C. L. Tan
Appl. Phys. Lett., v. 43, p. 415 (1983).

38. Wang, W. I., T. S. Kuan, E. E. Mendez and L. Esaki
Phys. Rev. B, v. 31, p. 6890 (1985).

39. Pérez-Álvarez, R., J. L. Parra-Santiago and P. Pajon-Suárez.
Physica Status Solidi (b), in press.

40. Pérez-Álvarez, R. and P. Pajon-Suárez
ICTP preprint IC/87/196.

41. Pérez-Álvarez, R. and P. Pajon-Suárez
Physica Status Solidi (b), in press.

NOTA: Trabajo presentado en el X SLAFES. (Diciembre de 1987)